

Evolution and microstructure of shear bands in nanostructured Fe

Q. Wei, D. Jia, K. T. Ramesh, and E. Ma^{a)}

Center for Advanced Metallic and Ceramic Systems (CAMCS), The Johns Hopkins University, Baltimore, Maryland 21218

(Received 6 March 2002; accepted for publication 25 June 2002)

Shear band development in consolidated nanocrystalline and ultrafine-grained Fe has been monitored as a function of overall strain from the onset of plastic deformation. The deformation mechanisms of the grains inside the shear bands, the origin of the inhomogeneous deformation, and the propensity for shear localization in nanostructures are explained based on microstructural information acquired using transmission electron microscopy. © 2002 American Institute of Physics. [DOI: 10.1063/1.1501158]

Nanostructured metals and alloys often exhibit unusual deformation behavior compared with their coarse-grained counterparts.¹ An example of this is the propensity for localized deformation in the form of shear banding.^{2–8} The most prominent cases of this phenomenon so far appear to be in bcc Fe and its alloys prepared through the powder metallurgy route.^{4–8} While pure Fe at conventional grain sizes (in the micrometer range) deforms uniformly in quasistatic tests over a range of plastic strains, shear banding is the dominant mode of plastic deformation when the grain sizes are in the nanocrystalline (nc) (<100 nm), and ultrafine-grained (UFG) (<300 nm) regime.^{8,9} We have attributed this instability to the diminishing strain hardening capacity and low strain rate sensitivity of the flow stress in these high-strength nc and UFG materials.^{8–10} However, little is known regarding the microscopic mechanisms responsible for triggering and sustaining the shear localization. In this letter, we describe an effort to monitor the development of shear bands as a function of plastic strain. Our focus is the examination of the microstructures inside the shear bands to improve our understanding of the processes by which the nc/UFG grains deform in forming the shear band.

Commercial pure iron powders with an average particle size of 5 μm were ball milled for 20 h in a SPEX 8000 mill in protective Ar atmosphere. The grains inside the particles were refined to 10–20 nm after milling.^{6,7,11} The powders were then consolidated into full density (>99%) compacts using a sinter-forging process (reported elsewhere).^{8,9} Depending on the consolidation temperature used, different average grain sizes ranging from 80 nm to many microns were obtained in the final product, as determined from a grain size distribution analysis in a transmission electron microscope (TEM). Rectangular samples (2.2×2.2×3.5 mm³) were tested in compression at a strain rate of 1×10^{-4} /s at room temperature. When the grain size is above $\sim 1 \mu\text{m}$, the plastic deformation takes place uniformly at least up to a plastic strain of about 15% over the entire sample. In sharp contrast, for grain sizes in the range of 80–300 nm, most of the plastic deformation is localized in narrow shear bands, often along

planes containing the highest shear stresses, as shown in Fig. 1.

Stress-strain curves from an Fe sample with an average grain size of 268 nm obtained in uniaxial compression for several load/unload/reload cycles are displayed in Fig. 1. The optical micrographs in the figure, taken after unloading at various levels of plastic strains, document the evolution of the shear band failure mode that accompanies the apparent strain softening. It is clear that shear localization sets in immediately after the onset of plastic deformation. With increasing strain, the existing bands widen slowly and new bands develop, eventually leading to a fairly dense network of shear bands with widths in the range of 2–20 μm . No void formation or cracking is visible at the intersections of the shear bands. In compression, a large plastic strain is achieved due to the development of multiple shear bands without fracture.

A tripod-polishing technique¹² was adapted and modified to solve the challenging problem of precisely locating the shear bands during TEM sample preparation and analysis. After obtaining perforation at the wedge edge near shear bands, the specimens were cleaned with a dual-gun ion mill at liquid nitrogen temperature. The TEM analysis was performed in a Philips EM-420 120 kV microscope. In addition, both electron energy loss spectroscopy and energy dispersive x-ray spectroscopy mapping were employed to rule out the segregation of impurities, using a Philips CM300 microscope equipped with a Gatan image filter system.

Figure 2(a) shows a bright-field TEM image taken outside a shear band and Fig. 2(b) shows an image inside the shear band. The TEM specimen was from a sample that has an average grain size of 110 nm and was tested to a nominal overall strain of 14%. It is seen that outside the shear band the Fe grains are by and large equiaxed. On the other hand, the grains inside the shear band are heavily elongated, with a very large true strain of the order of 2–3 and an average aspect ratio of ~ 10 , and often decorated with high densities of dislocations. Similar and even larger plastic strains are also known for the shear bands in amorphous metals. Selected area diffraction (SAD) from outside the band shows a uniform ring pattern corresponding to bcc Fe, with no evidence of preferential orientation of the grains. In contrast, the

^{a)}Electronic mail: ema@jhu.edu

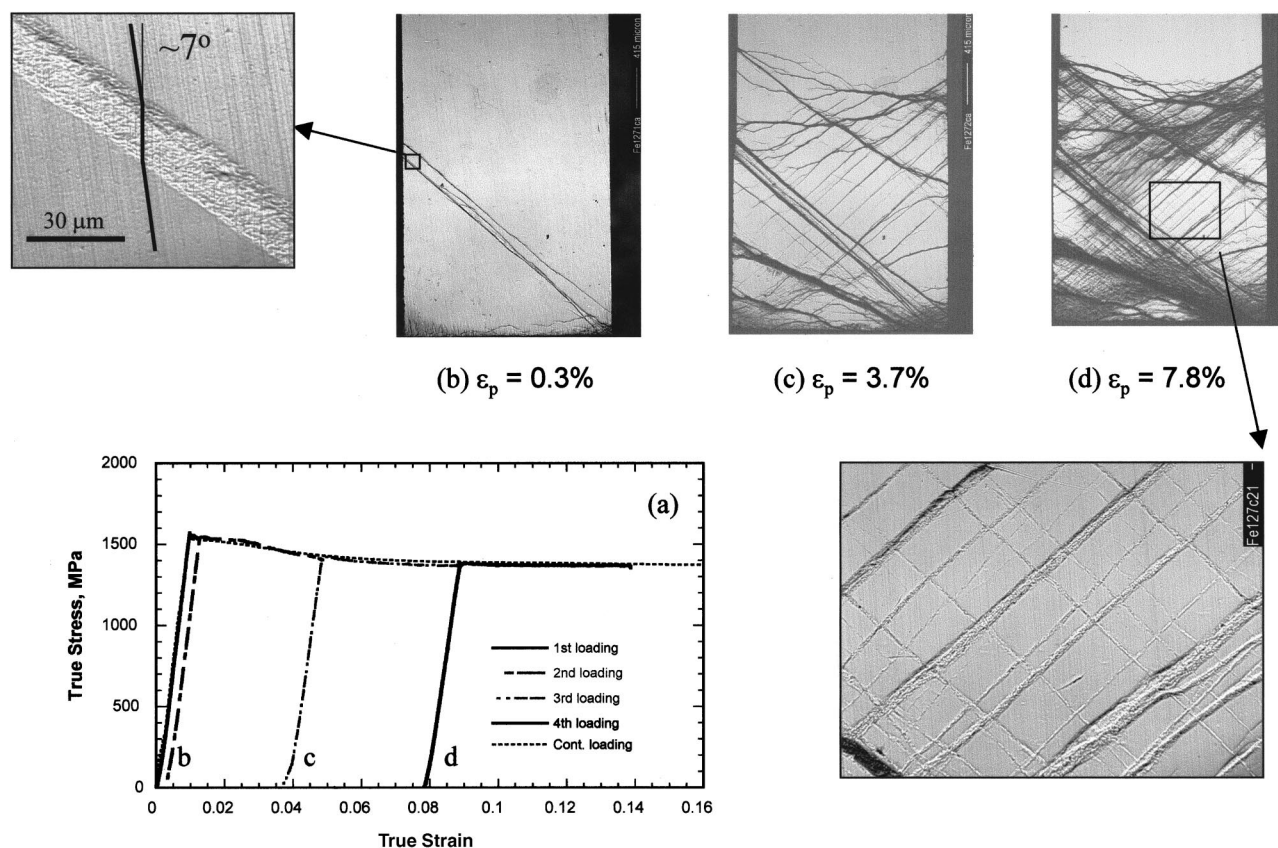


FIG. 1. A progressive compression test with loading, unloading, and reloading at various strain levels (0.3%, 3.7%, and 7.8%), showing the stress-strain behavior and the development of the shear bands. The Fe sample tested has an average grain size of 268 nm. Loading direction is vertical.

SAD pattern of the crystals inside the shear band [shown in Fig. 2(c)] shows strong maxima on the ring of $\{110\}$ reflections, indicating obvious texturing.¹³ Nonuniform rings can also be observed for other reflections. The sixfold symmetry observed in Fig. 2(c) suggests that the pattern is analogous to one that may be indexed as along the $\langle 111 \rangle$ zone axis. We therefore infer that the texturing inside the shear band involves the activation of the $\langle 111 \rangle / \{110\}$ slip systems of bcc Fe. Although slip systems of $\langle 111 \rangle / \{110\}$, $\langle 111 \rangle / \{112\}$, and $\langle 111 \rangle / \{123\}$ are all reported for bcc metals such as Ta, Mo, Cr,¹⁴ $\langle 111 \rangle / \{110\}$ appears to be almost the exclusive slip system for bcc Fe.¹⁵ The observations described in this paragraph indicate that, while our grain sizes (< 100 nm) are very close to being in the nanocrystalline regime, the large plastic deformation observed is clearly mediated by the conventional dislocation mechanisms.

The TEM images also suggest insignificant recrystallization and a nonadiabatic shear localization process. Other investigators have reported microstructures of shear bands in other bcc as well as fcc and hcp metals, such as Ta, Cu, Ti^{16–22} in which the shear bands were typically adiabatic, developed under high-rate loading. TEM in such cases typically reveals a gradient of microstructure across the shear band. Much finer grains (a refinement sometimes by one order of magnitude) with equiaxed geometry and no texturing have been observed inside such shear bands, as compared to the grain structure outside the shear bands. Such observations have in the past been attributed to recrystallization due to either a significant temperature rise or due to very large

plastic deformations (see Ref. 23 for a discussion). Our shear bands are clearly very different in all the earlier aspects. The uniform microstructure across the band, with sharp boundaries, is shown in Fig. 3.

Some of the grains inside the shear band appear to have relatively large volumes. A closer look (micrograph not shown) inside such grains, however, revealed small-angle boundaries that might have evolved from the originally high-angle ones. In other words, the grains have experienced rotations and alignment in forming the band with texture, allowing easy slip propagation in certain orientations. It is expected that after the severe deformation the grains inside the shear band would be oriented for maximum shear stress in their $\langle 111 \rangle / \{110\}$ slip systems. It is conceivable that such cooperative deformation across the band is easier when it involves many tiny grains rather than large grains, possibly explaining the enhanced propensity for shear localization when the grain size is in the nc/UFG regime.

In summary, we have shown that consolidated nc or UFG Fe is prone to plastic instability, with shear localization becoming the primary mode from the onset of plastic deformation. The microstructures inside the shear bands indicate dislocation-based mechanisms for the large deformation of the nc grains, and suggest geometric rather than adiabatic softening as the origin for the inhomogeneous deformation. We believe that it is the small sizes of the nc/UFG grains that make it possible for a large group of grains to quickly develop the texturing favorable for slip propagation in a cooperative manner, facilitating the localization of the plastic deformation.

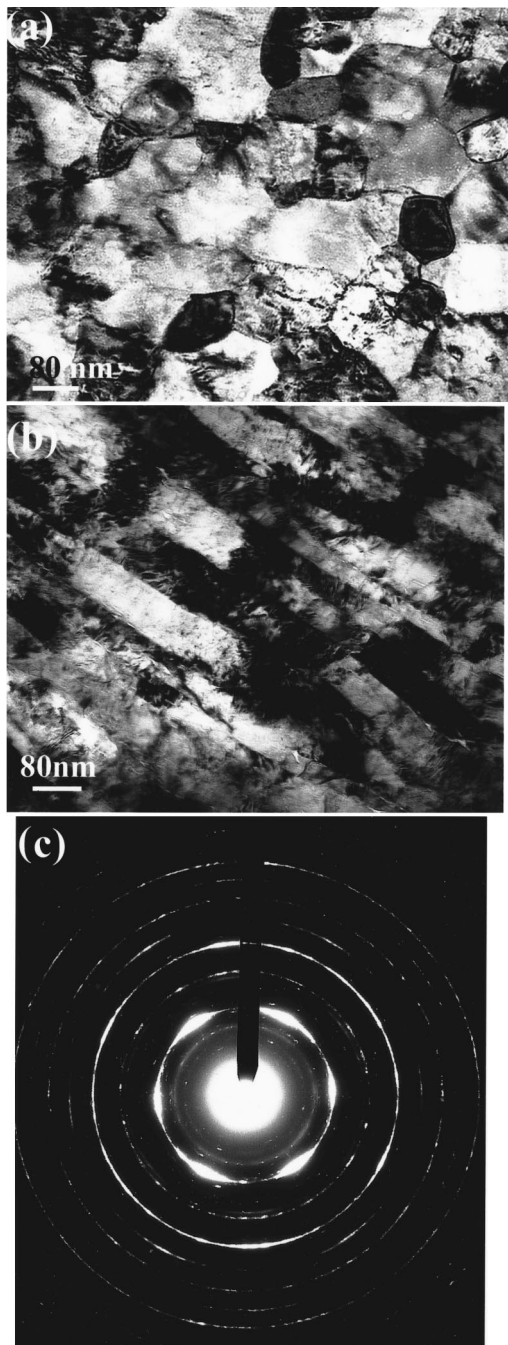


FIG. 2. Bright-field TEM images of (a) the equiaxed grains outside a shear band contrasted with (b) elongated grains inside a shear band. Also see Fig. 3 for an encompassing view of these grain structures. The SAD pattern in (c) is taken inside the shear band. The average grain size of the as-consolidated sample is 110 nm.

formation. Due to the lack of strain hardening except at small plastic strains and strain rate hardening in nc/UFG metals,^{8–10} many of these strong materials are likely to develop the shear banding instability under certain loading/sample conditions.^{4–10}

This work was performed under the auspices of CAMCS at Johns Hopkins, sponsored by the Army Research Labora-

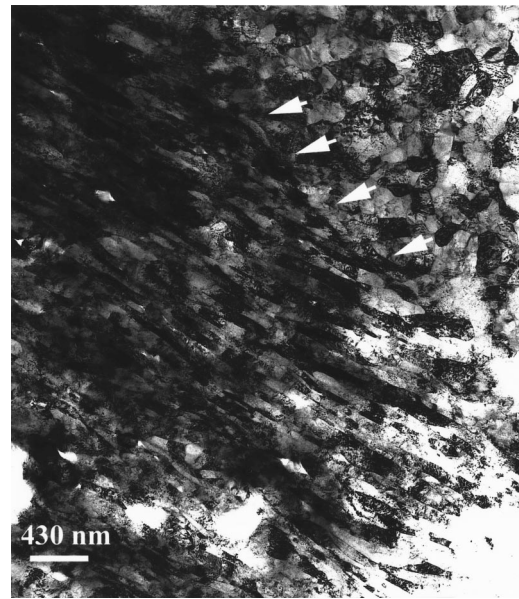


FIG. 3. Bright-field TEM image showing the uniform microstructure inside the band and relatively sharp boundary (marked by arrows) of a shear band.

tory under the ARMAC–RTP Cooperative Agreement No. DAAD19-01-2-0003. E.M. is also supported by NSF-CMS-9877006.

- ¹H. Gleiter, *Acta Metall.* **48**, 1 (2000).
- ²A. B. Witney, P. G. Sanders, J. R. Weertman, and J. A. Eastman, *Scr. Metall. Mater.* **33**, 2025 (1995).
- ³P. G. Sanders, C. J. Youngdahl, and J. R. Weertman, *Mater. Sci. Eng., A* **234–236**, 809 (1997).
- ⁴J. E. Carsley, W. W. Milligan, S. A. Hackney, and E. C. Aifantis, *Metall. Trans. A* **26A**, 2479 (1995).
- ⁵J. E. Carsley, W. W. Milligan, S. A. Hackney, and E. C. Aifantis, *Metall. Mater. Trans. A* **29A**, 2261 (1998).
- ⁶T. R. Malow and C. C. Koch, *Metall. Mater. Trans. A* **29A**, 2285 (1998).
- ⁷T. R. Malow, C. C. Koch, P. Q. Miraglia, and K. L. Murty, *Mater. Sci. Eng., A* **252**, 36 (1998).
- ⁸D. Jia, K. T. Ramesh, and E. Ma, *Scr. Mater.* **42**, 73 (2000).
- ⁹D. Jia, K. T. Ramesh, and E. Ma (unpublished).
- ¹⁰D. Jia, Y. M. Wang, K. T. Ramesh, E. Ma, Y. T. Zhu, and R. Z. Valiev, *Appl. Phys. Lett.* **79**, 611 (2001).
- ¹¹J. Eckert, J. C. Holzer, C. E. Krill III, and W. L. Johnson, *J. Mater. Res.* **7**, 1751 (1992).
- ¹²J. Ayache and P. H. Albarede, *Ultramicroscopy* **60**, 195 (1995).
- ¹³C. S. Barrett, *Structure of Metals* (McGraw-Hill, New York, 1952), p. 442.
- ¹⁴S. Nemat-Nasser, T. Okinaka, and L. Ni, *J. Mech. Phys. Solids* **46**, 1009 (1998).
- ¹⁵M. S. Duesberry and V. Vitek, *Acta Mater.* **46**, 1481 (1998).
- ¹⁶Y. B. Xu, W. L. Zhong, Y. J. Chen, L. T. Shen, Q. Liu, Y. L. Bai, and M. A. Meyers, *Mater. Sci. Eng., A* **299**, 287 (2001).
- ¹⁷V. F. Nesterenko, M. A. Meyers, J. C. LaSalvia, M. P. Bondar, Y. J. Chen, and Y. L. Lukyanov, *Mater. Sci. Eng., A* **229**, 23 (1997).
- ¹⁸M. T. Perez-Prado, J. A. Hines, and K. S. Vecchio, *Acta Mater.* **49**, 2905 (2001).
- ¹⁹M. A. Meyers, G. Subbush, B. K. Kad, and L. Prasad, *Mech. Mater.* **17**, 175 (1994).
- ²⁰U. Andrade, M. A. Meyers, K. S. Vecchio, and A. H. Chokshi, *Acta Metall. Mater.* **42**, 3183 (1994).
- ²¹D. R. Chichili, K. T. Ramesh, and K. Hemker, *Acta Mater.* **46**, 1025 (1998).
- ²²D. R. Chichili and K. T. Ramesh, *J. Appl. Mech.* **66**, 10 (1999).
- ²³J. A. Hines, K. S. Vecchio, and S. Ahzi, *Metall. Mater. Trans. A* **29A**, 191 (1998).